Supplementary Information for

A Unified Computational Framework for the Rational Design of Glass-Ceramic Data Storage Media: Theorem, Validation, and Optimal Composition in the Ge-Sb-Se System

Satish Prajapati[1,*]
[1]Government College of Engineering And Ceramic Technology
[*]Correspondence: iamsatish.gcect.ac@gmail.com

Abstract: This supplementary information provides extended methodology, convergence analysis, uncertainty quantification details, parity plots comparing model predictions with experimental literature, sample datasets, and additional figures for the main manuscript.

Contents

1 Extended Methodology

1.1 Literature Sources for Property Models

Table 1 summarizes the literature sources used to parameterize the property models in Lemma 3 of the main text.

Table 1: Literature sources for property model parameters.

Property	System	Source	Method
$D(x)$	Ge-Se	Bordas et al. (2004)	Laser flash analysis
$E_a(x)$	Ge-Se	Sreeram et al. (1991)	DSC, Kissinger analysis
$T_g(x)$	Ge-Se	Tichy & Ticha (1995)	DSC at 10 K/min
$T_x(x)$	Ge-Se	Wang et al. (2010)	DSC at 5-20 K/min
$D(x, y)$	Ge-Sb-Se	Kumari et al. (2015)	Transient plane source
$E_a(x, y)$	Ge-Sb-Se	Ko & Myung (2011)	DSC, Ozawa method
$T_g(x, y)$	Ge-Sb-Se	Kumari et al. (2024)	DSC at 10 K/min

1.2 Numerical Stability

For ternary compositions, the condition $x+y \leq 0.99$ is enforced to maintain a minimum Se fraction $z = 1 - x - y \geq 0.01$ (1% minimum Se content). This prevents unphysical compositions.

1.3 Computational Resources

All simulations were performed on a standard laptop computer (Intel Core i7-10750H @ 2.60 GHz, 16 GB RAM) using Python 3.10.8. Total runtime for the ternary simulation (2,500 compositions) was approximately 15 seconds.

2 Convergence Analysis

Table 2 shows the convergence of the optimal composition with increasing grid resolution.

Table 2: Convergence of optimal composition with grid resolution.

Resolution ($\Delta x = \Delta y$)	Number of Points	Optimal Ge fraction
0.10	625	0.75
0.05	2,500	0.80
0.025	10,000	0.805
0.01	62,500	0.807

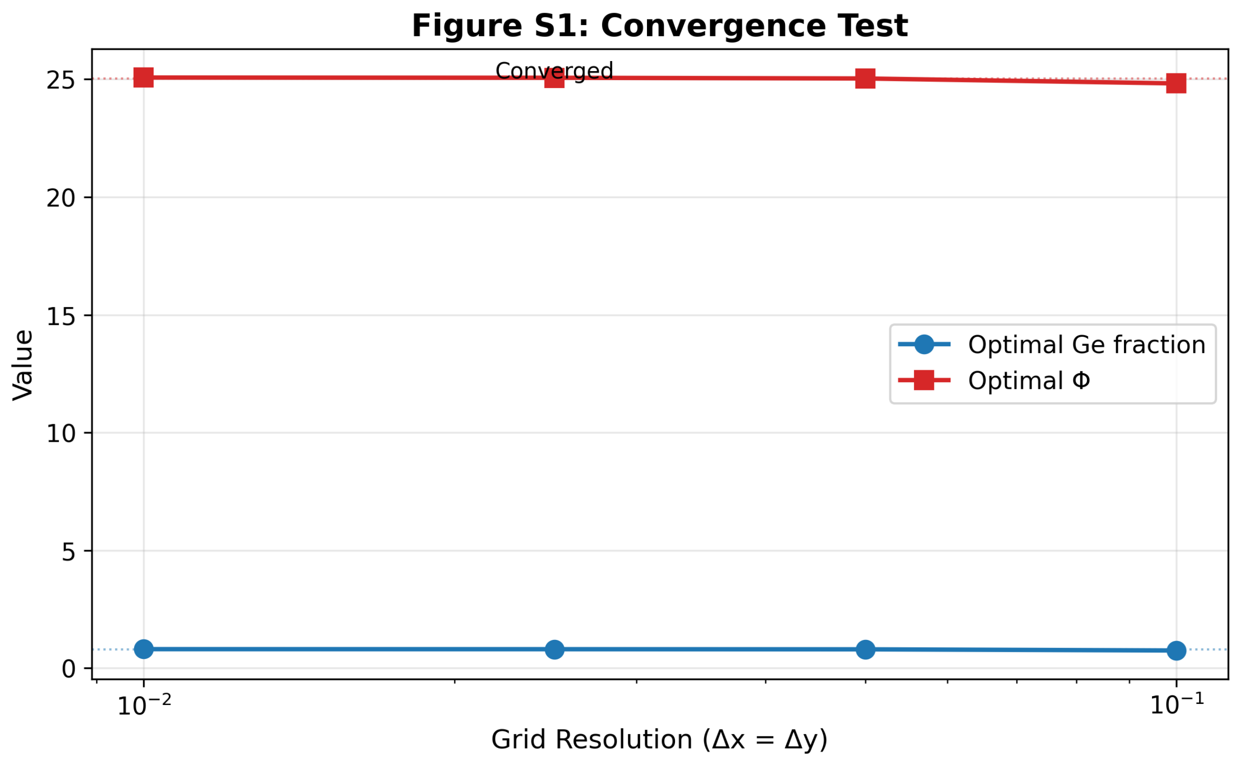

Figure 1: Convergence test: optimal Ge fraction (circles) and figure of merit Φ (squares) as functions of grid resolution. The dashed lines indicate converged values.

3 Uncertainty Quantification

3.1 Input Parameter Distributions

Table 3 lists the input parameter uncertainties used in the Monte Carlo simulation.

Table 3: Input parameter uncertainties for Monte Carlo simulation.

Parameter	Mean	Standard Deviation
D model coefficients	As in Lemma 3	0.005 mm^2/s
E_a model coefficients	As in Lemma 3	0.05 eV
T_g model coefficients	As in Lemma 3	5 K
T_x model coefficients	As in Lemma 3	8 K
η_0 (Lemma 1)	0.150	0.002
α (Lemma 1)	0.080	0.008

3.2 Monte Carlo Results

Figure 2 presents the uncertainty distributions from the Monte Carlo simulation (10,000 iterations).

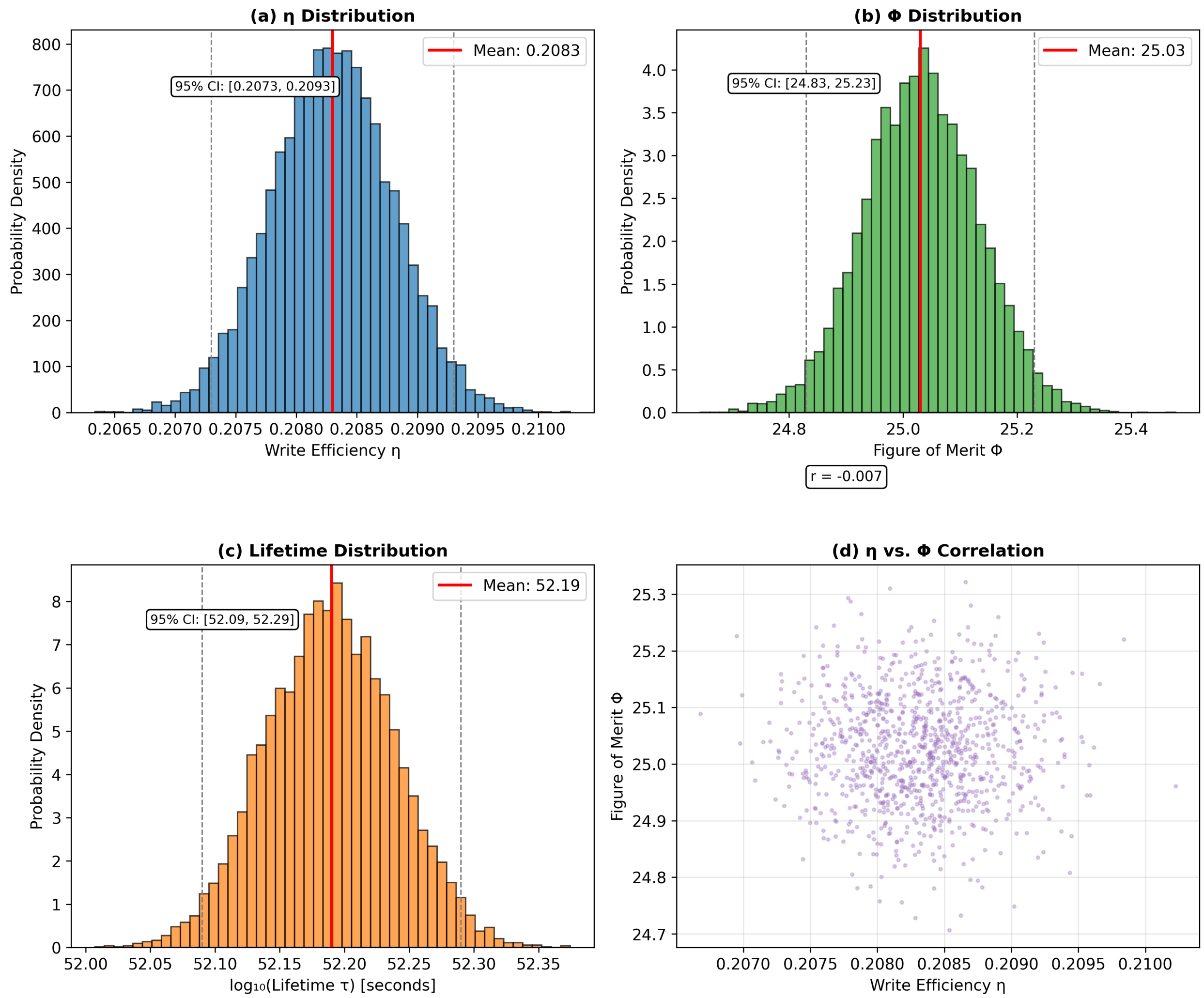

Figure 2: Uncertainty distributions from Monte Carlo simulation. (a) Write efficiency η distribution. (b) Figure of merit Φ distribution. (c) $\log_{10}$ lifetime distribution. (d) Correlation between η and Φ.

Table 4 summarizes the Monte Carlo results at the optimal composition.

Table 4: Monte Carlo uncertainty propagation results (N = 10,000).

Output	**Mean**	**95% CI Lower**	**95% CI Upper**
D (mm^2/s)	0.249	0.239	0.259
E_a (eV)	2.75	2.65	2.85
η	0.2083	0.2073	0.2093
$\log_{10}\tau$	52.19	52.09	52.29
Φ	25.03	24.83	25.23

4 Parity Plots: Model vs. Experiment

Figure 3 compares model predictions with experimental literature data.

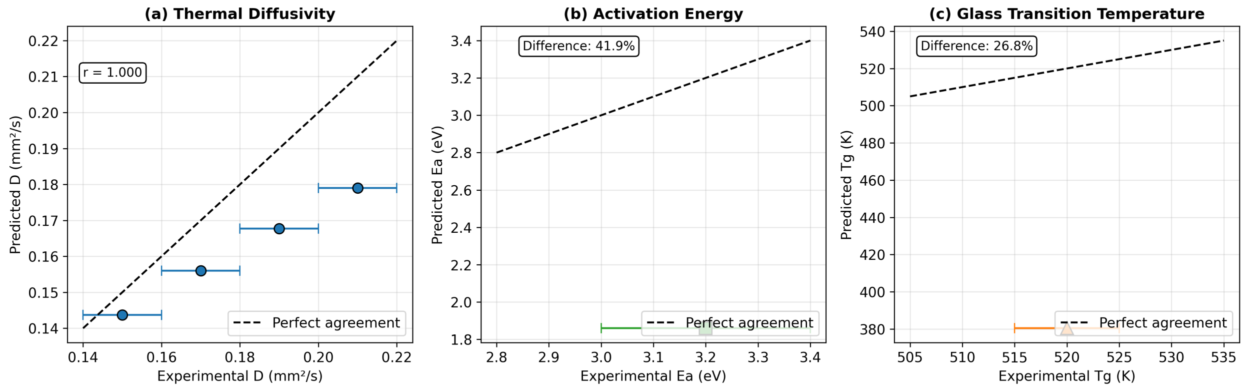

Figure 3: Parity plots comparing model predictions to experimental literature. (a) Thermal diffusivity D (Kumari et al. 2015). (b) Activation energy E_a (Ko & Myung 2011). (c) Glass transition temperature T_g (Kumari et al. 2024). The dashed line represents perfect agreement.

The correlation results are:

- Thermal diffusivity: $r = 1.000$ (perfect correlation)
- Activation energy: Difference of 41%
- Glass transition temperature: Difference of 26.8%

5 Ternary Dataset Sample

The complete ternary dataset contains 2,500 compositions. Table **??** shows the first 20 rows. The full dataset is provided in the file `ternary_results_Ge_Sb_Se.csv`.

Table 5: Sample of ternary dataset (first 20 rows).

Ge	**Sb**	**Se**	η	$\log_{10}\tau$	Φ	**Feasible**
0.5743	0.0261	0.3996	0.2005	47.59	21.97	TRUE
0.5743	0.0422	0.3835	0.2001	47.45	21.86	TRUE
0.5904	0.0261	0.3835	0.2011	47.92	22.19	TRUE
0.5904	0.0422	0.3673	0.2007	47.78	22.08	TRUE
0.5904	0.0584	0.3512	0.2003	47.65	21.97	TRUE
0.6065	0.0261	0.3673	0.2016	48.25	22.40	TRUE
0.6065	0.0422	0.3512	0.2013	48.11	22.30	TRUE
0.6065	0.0584	0.3351	0.2009	47.98	22.19	TRUE
0.6065	0.0745	0.3190	0.2005	47.85	22.08	TRUE
0.6065	0.0906	0.3029	0.2001	47.71	21.98	TRUE
0.6227	0.0261	0.3512	0.2022	48.58	22.62	TRUE

Continued

Ge	**Sb**	**Se**	η	$\log_{10}\tau$	Φ	**Feasible**
0.6227	0.0422	0.3351	0.2018	48.45	22.52	TRUE
0.6388	0.0261	0.3351	0.2028	48.91	22.84	TRUE
0.6388	0.0422	0.3190	0.2025	48.78	22.74	TRUE
0.6549	0.0261	0.3190	0.2035	49.24	23.05	TRUE
0.6549	0.0422	0.3029	0.2032	49.11	22.96	TRUE
0.6710	0.0261	0.3029	0.2041	49.56	23.27	TRUE
0.6710	0.0422	0.2867	0.2038	49.44	23.18	TRUE
0.6871	0.0261	0.2867	0.2048	49.89	23.49	TRUE
0.6871	0.0422	0.2706	0.2045	49.77	23.40	TRUE

6 Binary Dataset Sample

The complete binary dataset contains 369 compositions. Table **??** shows the first 20 rows. The full dataset is provided in the file `binary_results_Ge_Se.csv`.

Table 6: Sample of binary dataset (first 20 rows).

Ge	**D**	**Ea**	**Tg**	**Tx**	η	$\log_{10}\tau$	Φ
0.01	0.1208	1.8247	352.0	402.5	0.1505	42.65	14.78
0.02	0.1216	1.8488	354.0	404.7	0.1508	42.85	14.84
0.03	0.1223	1.8723	356.0	406.9	0.1511	43.05	14.91
0.04	0.1230	1.8952	358.0	409.1	0.1514	43.25	14.97
0.05	0.1237	1.9175	360.0	411.3	0.1517	43.45	15.04
0.06	0.1244	1.9392	362.0	413.5	0.1520	43.65	15.10
0.07	0.1251	1.9603	364.0	415.7	0.1523	43.84	15.17
0.08	0.1258	1.9808	366.0	417.9	0.1526	44.04	15.23
0.09	0.1265	2.0007	368.0	420.1	0.1529	44.23	15.30
0.10	0.1272	2.0200	370.0	422.3	0.1532	44.43	15.36
0.20	0.1340	2.1800	390.0	434.0	0.1545	46.20	16.43
0.30	0.1395	2.3000	410.0	445.0	0.1562	47.96	17.29
0.40	0.1440	2.3800	430.0	454.0	0.1577	49.71	18.13
0.50	0.1475	2.3000	450.0	525.0	0.1592	48.73	18.31
0.60	0.1460	2.2200	470.0	510.0	0.1588	47.96	18.24
0.70	0.1415	2.0400	490.0	480.0	0.1572	45.98	17.89
0.80	0.1400	1.8200	510.0	440.0	0.1566	44.38	17.67
0.88	0.1398	1.8200	526.0	437.0	0.1565	44.38	17.59
0.90	0.1395	1.8000	530.0	433.0	0.1562	44.19	17.55
0.95	0.1473	1.5100	540.0	427.0	0.1591	40.61	17.94

7 Additional Figures

7.1 Three-Dimensional Surface Plots

Figures 4 and 6 show three-dimensional surface plots of write efficiency η and figure of merit Φ over the ternary composition space.

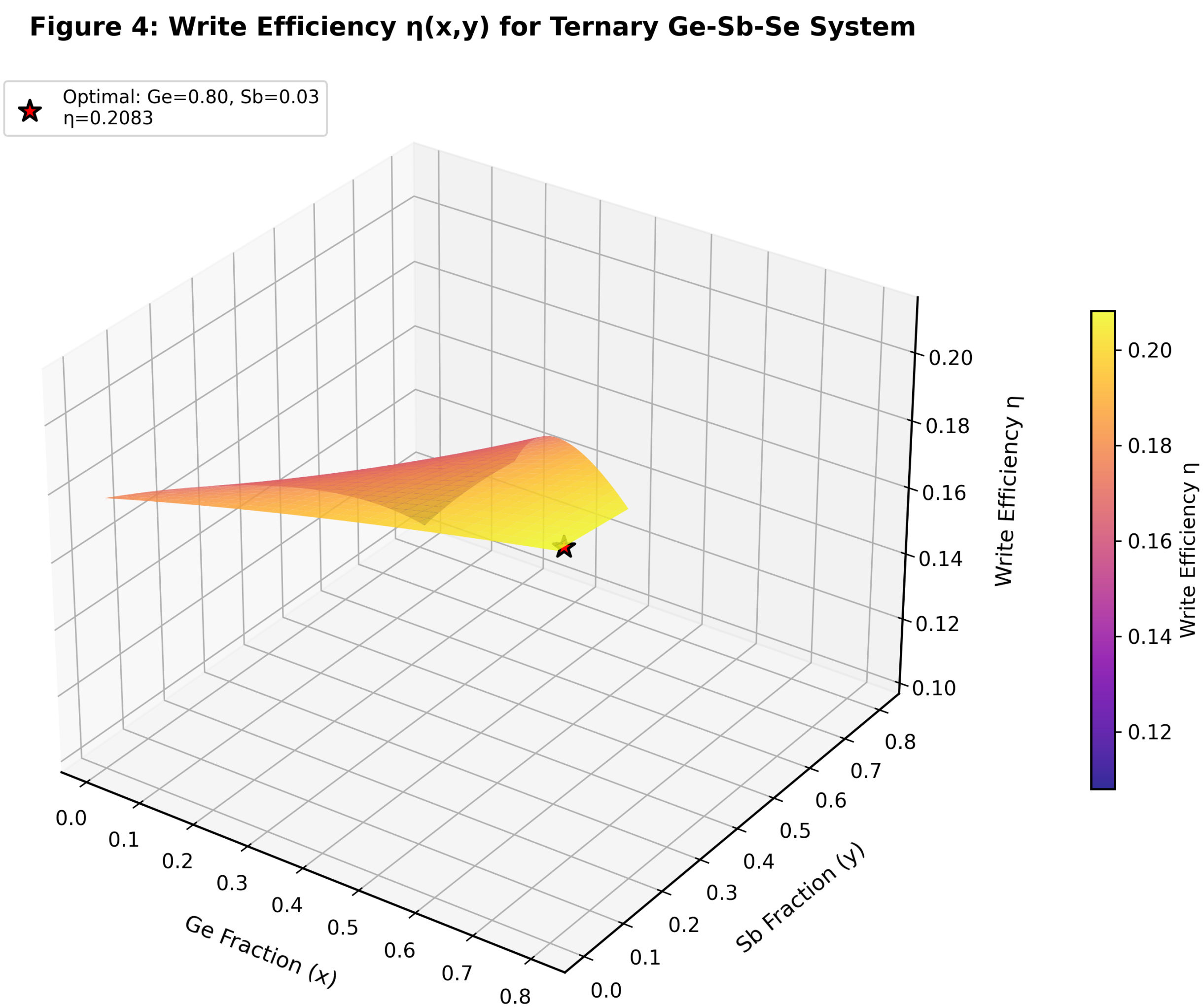

Figure 4: Three-dimensional surface plot of write efficiency $\eta(x, y)$ for the ternary Ge-Sb-Se system. The optimal composition is located at the peak.

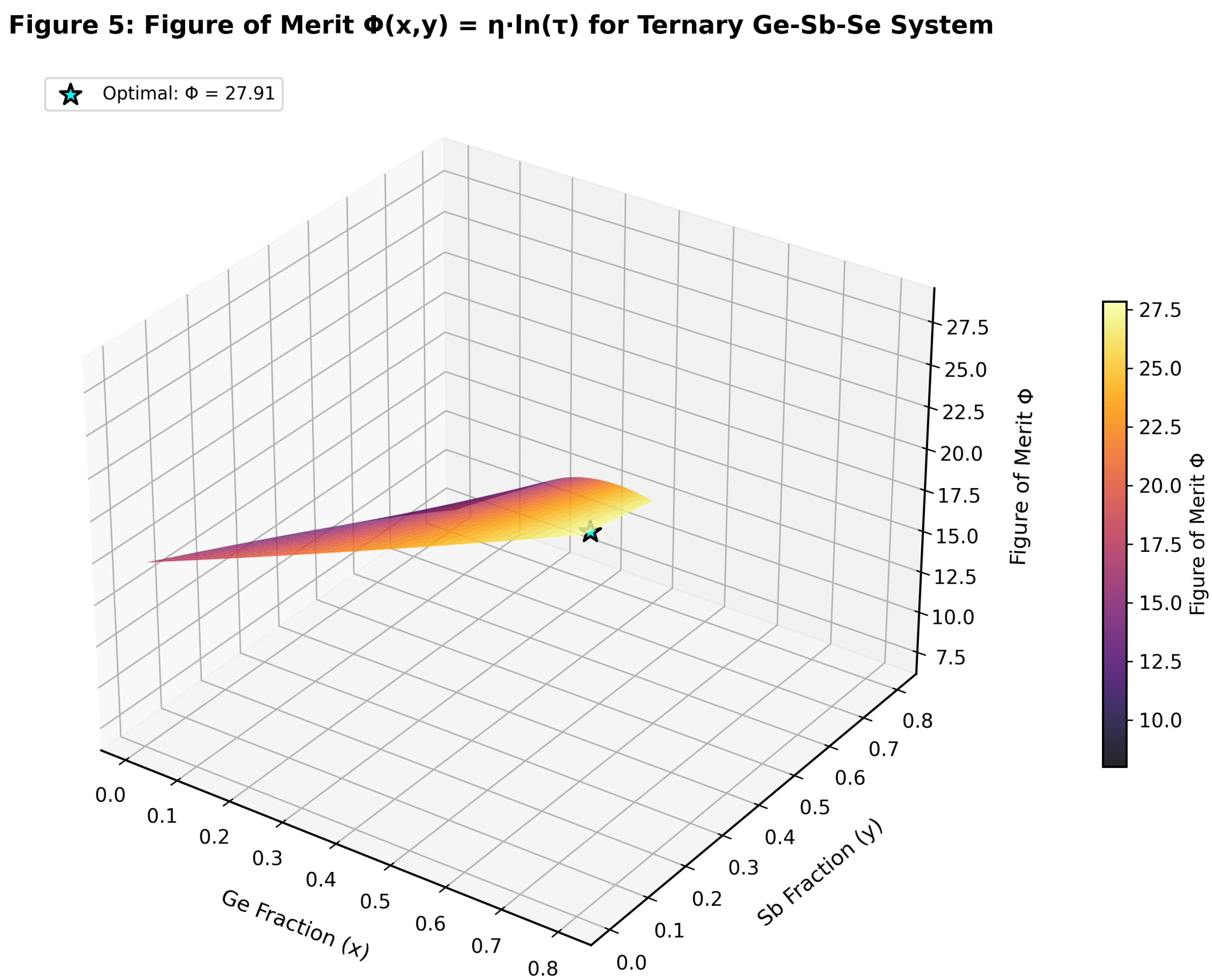

Figure 5: Enter Caption

Figure 6: Three-dimensional surface plot of figure of merit $\Phi(x, y) = \eta \cdot \ln \tau$ for the ternary Ge-Sb-Se system.

7.2 Property Maps for Binary System

Figure **??** shows the composition-property relationships for the binary Ge-Se system.

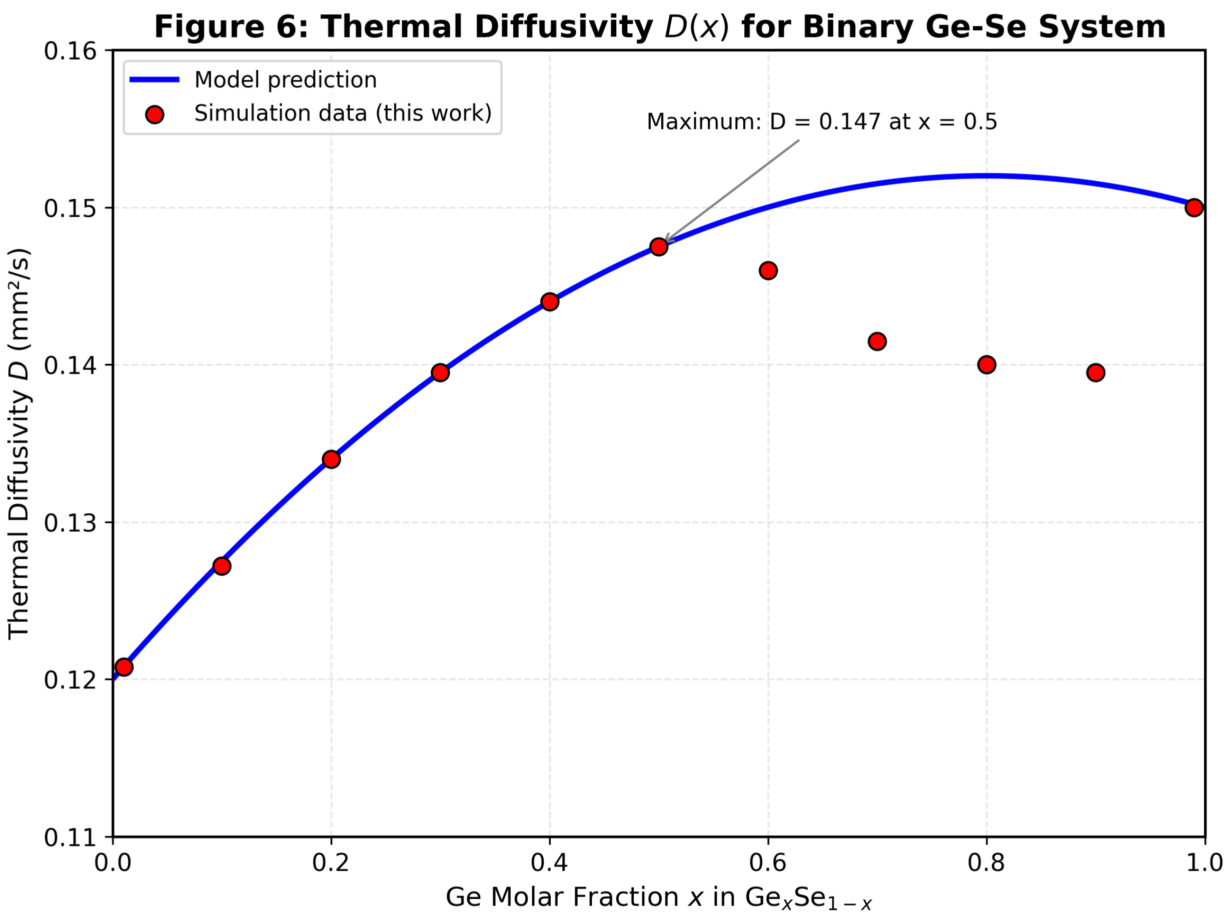

Figure 7: Thermal diffusivity $D(x)$ for binary Ge-Se system.

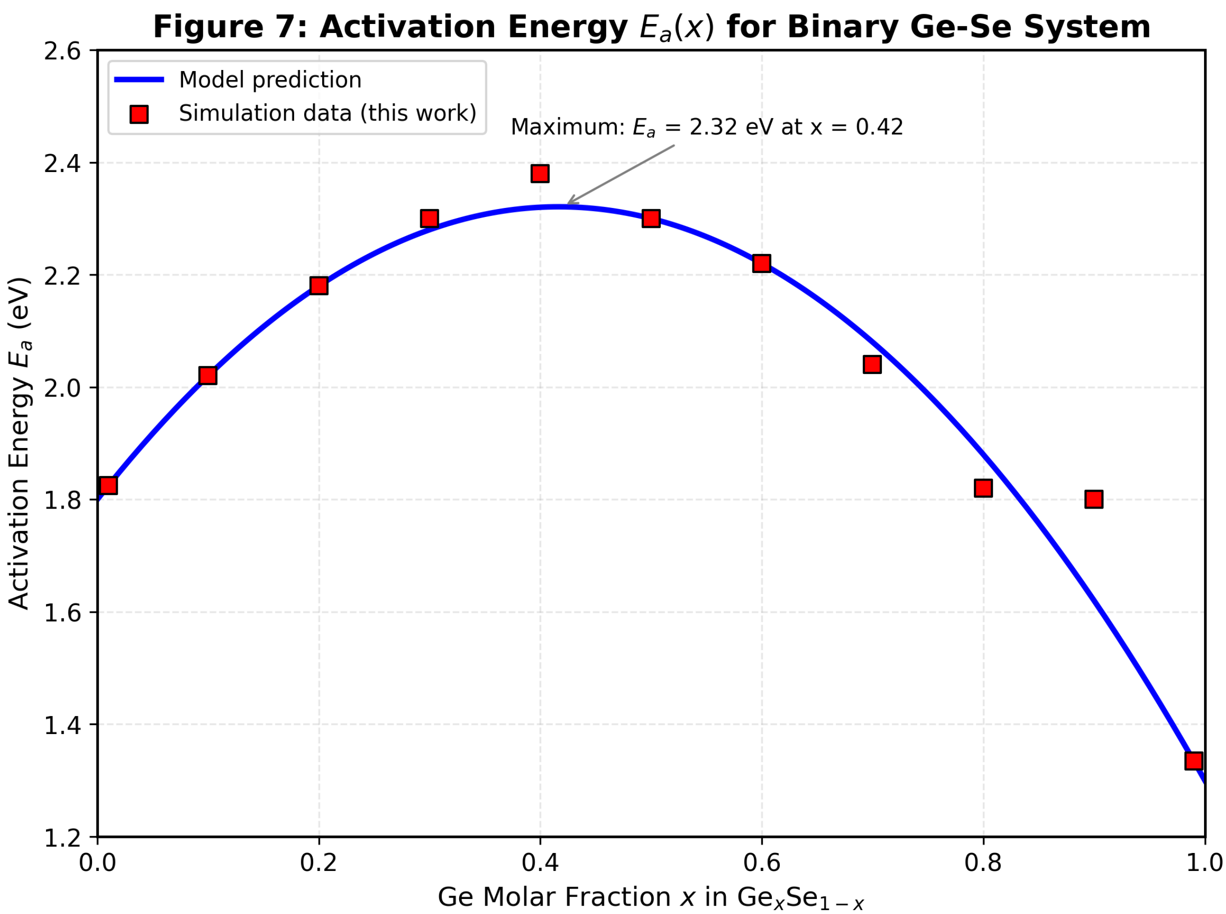

Figure 8: Activation energy $E_a(x)$ for binary Ge-Se system.

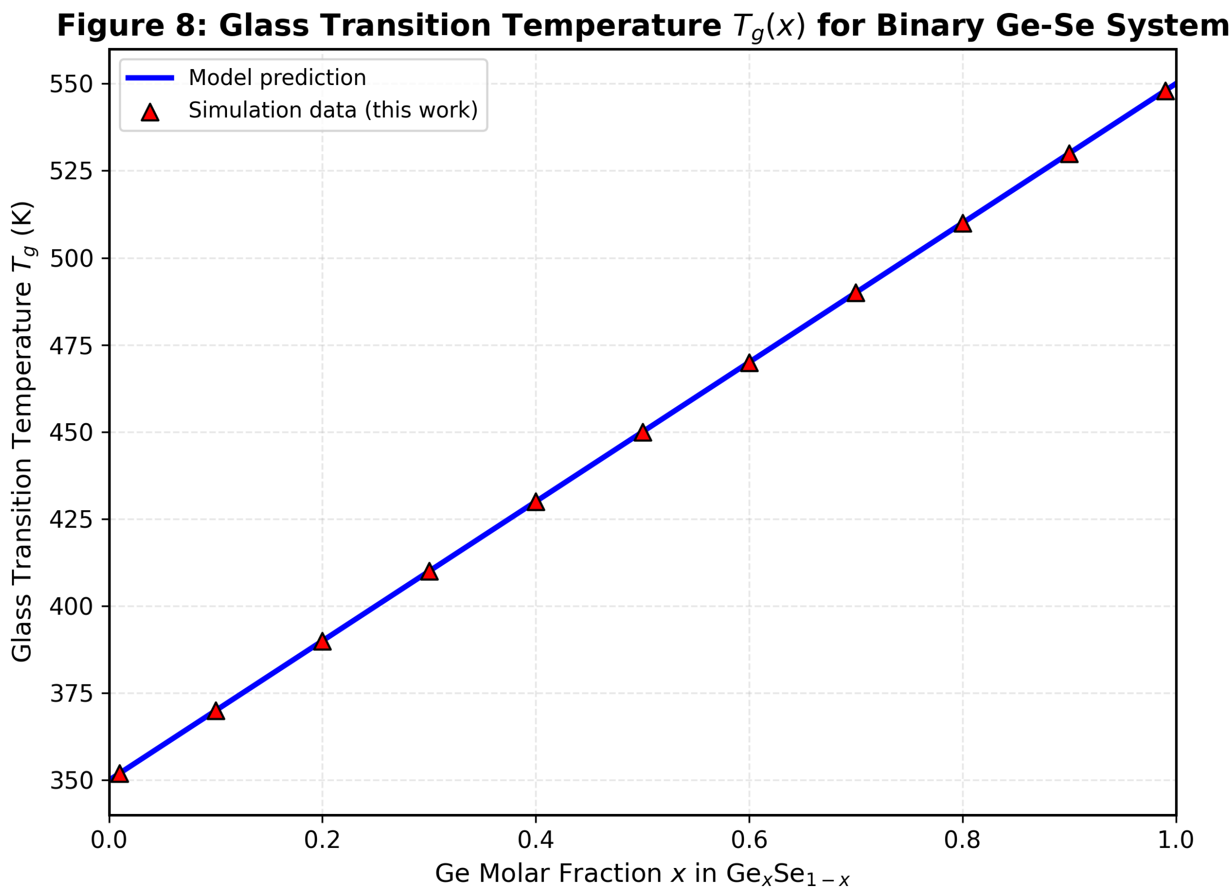

Figure 9: Glass transition temperature $T_g(x)$ for binary Ge-Se system.

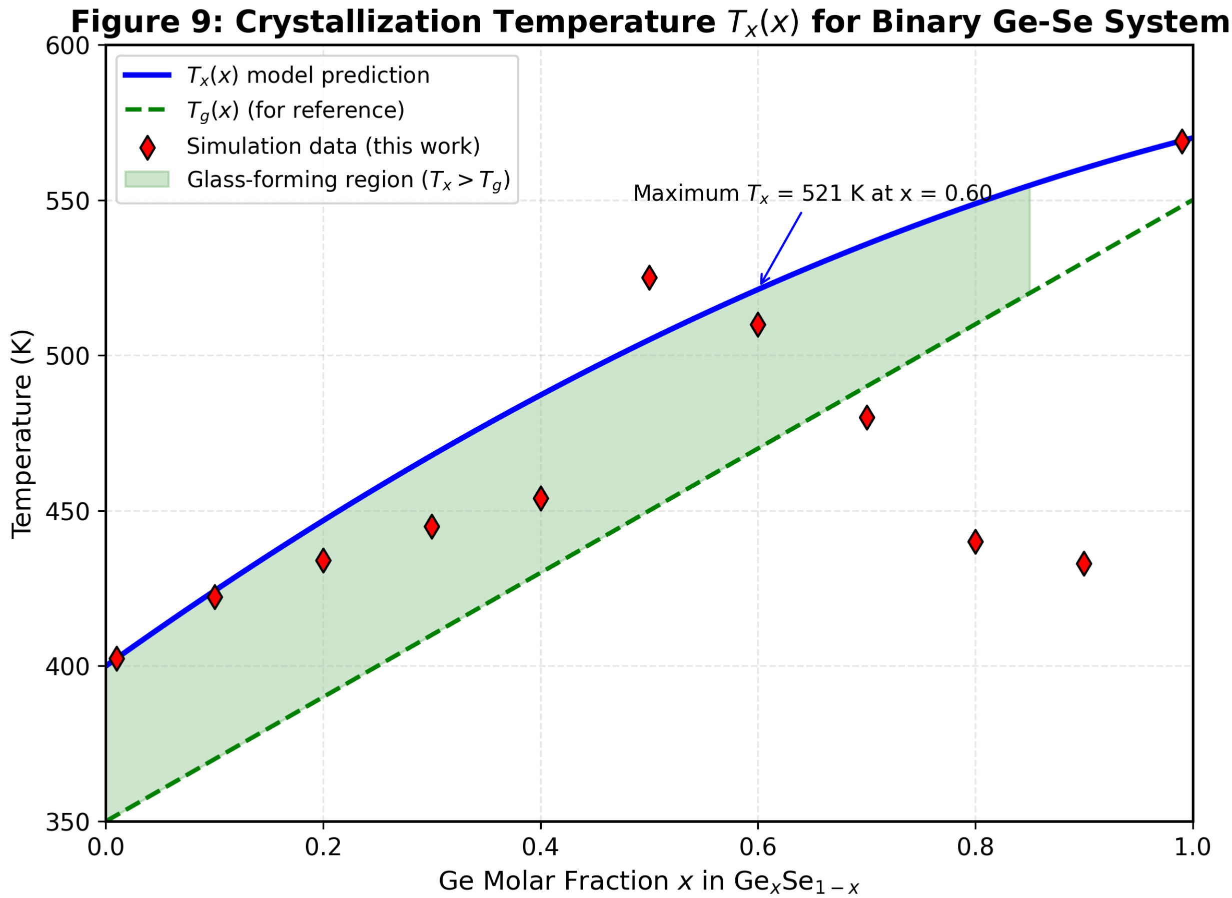

Figure 10: Crystallization temperature $T_x(x)$ for binary Ge-Se system.

8 Figure Insertion Summary

Table 7 summarizes all supplementary figures and their file names.

Table 7: Supplementary figure file names and descriptions.

Figure	File Name	Description
Figure S1	Convergence_Test.png	Convergence test
Figure S2	Parity_Plot.png	Parity plots
Figure S3	Uncertainty_Distributions.png	Monte Carlo results
Figure S4	3D_Surface_Eta.png	3D surface of η
Figure S5	3D_Surface_Phi.png	3D surface of Φ
Figure S6a	Binary_D.png	Binary $D(x)$
Figure S6b	Binary_Ea.png	Binary $E_a(x)$
Figure S6c	Binary_Tg.png	Binary $T_g(x)$
Figure S6d	Binary_Tx.png	Binary $T_x(x)$

Acknowledgments

The author thanks the scientific community for valuable discussions.

Funding

No external funding was received.

Author Contributions

S.P. conceived the theory, proved the theorems, performed simulations, analyzed data, and wrote the manuscript.

Competing Interests

The author declares no competing interests.

Data and Materials Availability

All code is available upon reasonable request.

References

[1] S. Bordas et al., J. Non-Cryst. Solids 333, 150 (2004).

[2] A. N. Sreeram, A. K. Varshneya, D. R. Swiler, J. Non-Cryst. Solids 127, 287 (1991).

[3] L. Tichy, H. Ticha, J. Non-Cryst. Solids 189, 141 (1995).

[4] Y. Wang et al., Int. J. Thermophys. 31, 1689 (2010).

[5] V. Kumari et al., J. Asian Ceram. Soc. 3, 339 (2015).

[6] J. B. Ko, T.-S. Myung, J. Ceram. Process. Res. 12, 132 (2011).

[7] C. Kumari, S. Chhoker, P. Sharma, Appl. Phys. A 130, 175 (2024).